NBS TECHNICAL NOTE 517

Accelerometer Calibration With the Earth's Field Dynamic Calibrator

U.S. DEPARTMENT OF COMMERCE
National Bureau of Standards

UNITED STATES DEPARTMENT OF COMMERCE
Maurice H. Stans, Secretary
NATIONAL BUREAU OF STANDARDS • Lewis M. Branscomb, Director

NBS TECHNICAL NOTE 517

ISSUED MARCH 1970

Nat. Bur. Stand. (U.S.), Tech. Note 517, 30 pages (Mar. 1970)
CODEN: NBTNA

Accelerometer Calibration With the Earth's Field Dynamic Calibrator

John S. Hilten

Electronic Technology Division
Institute for Applied Technology
National Bureau of Standards
Washington, D.C. 20234

For sale by the Superintendent of Documents, U.S. Government Printing Office, Washington, D.C., 20402.
(Order by SD Catalog No. C 13.46:517). Price 35 cents.

Contents

List of Tables

List of Figures

Accelerometer Calibration with the Earth's Field Dynamic Calibrator*

John S. Hilten

This paper describes a simple device for the precise dynamic calibration of certain accelerometers at low frequencies. Calibration of an accelerometer is achieved by rotating the instrument in the earth's gravitational field at a number of constant rotational speeds.

Key words: Accelerometer; air bearings; calibrator, accelerometer; dynamic; earth's field; InterAgency Transducer Project; low frequency; rotational frequency response; transducer.

1. Introduction

Calibration of accelerometers for the measurement of time-varying accelerations is generally accomplished by use of an electromagnetic shaker to apply sinusoidal excitation to the accelerometer. Accuracy of the calibration data obtained by this means is limited by the accuracy with which the motion of the shaker is known.

The earth's gravitational field offers a precisely known acceleration for the static calibration of accelerometers. In 1954 Wildhack and Smith[1] investigated the application of this known field to dynamic calibration, and constructed for this purpose a device that would rotate an accelerometer in a vertical plane at known speeds, thus subjecting it to sinusoidal acceleration of 1g amplitude (g = 9.80665 m/s^2). This scheme has two major advantages: the applied acceleration is precisely known and constant, and it is possible to obtain a precise static calibration of the instrument in the same setup. A valid method for dynamic calibration should produce values that approach identity with the static calibration values as the frequency of excitation is lowered.

Such a technique is of particular value for the calibration of high precision accelerometers with negligible transverse response, such as servo types, which respond to steady state accelerations. This paper describes the test results obtained during the calibration of three instruments of this type.

In addition, this technique was used for the calibration of two strain-gage accelerometers with very low natural frequencies.

* The work was performed as part of a project on development of methods for evaluation of electro-mechanical transducers. The project has been jointly supported by a number of government agencies, including USN, USA, USAF and NASA. During the period of performance of this work, the Project Leader was Paul S. Lederer.

[1] W. A. Wildhack and R. O. Smith, A Basic Method of Determining the Dynamic Characteristics of Accelerometers by Rotation, Paper No. 54-40-3, Instrument Society of America, 1954.

2. Theory

The Wildhack-Smith paper describes three forces that act on the seismic mass of an accelerometer under calibration on the earth's field dynamic calibrator:

(1) Orientation Component - The $\pm 1g$ sinusoidal component of gravitational acceleration applied to the instrument. This is given in the following equation,

$$A_1 = g \text{ Sine } \theta,$$

where A_1 = the sinusoidal acceleration being applied to the instrument,

g = the acceleration due to gravity, and

θ = the angle between the accelerometer's sensitive axis and the direction of the earth's gravitational field.

(2) Constant Centrifugal Component - Since in any practical case the center of gravity of the accelerometer's seismic mass (zero acceleration position) will not exactly coincide with the axis of rotation of the calibrator, there will be a constant centrifugal component. The effect of this constant component disappears if the instrument is linear.

(3) Sinusoidal Centrifugal Component - As the seismic mass of the accelerometer under calibration moves sinusoidally due to the gravity or orientation component described in (1), it is also acted upon by the centrifugal field of the calibrator test table. The result is a sinusoidal component which varies with the square of the rotational speed of the calibrator. It should be noted that the small displacement associated with a high natural frequency reduces the magnitude of this component.

It is evident from the foregoing that the calibration of an accelerometer on a rotary calibrator will not generate the familiar, linear, single degree of freedom phase and amplitude frequency-response curves; instead a new family of curves is generated. The two equations below taken from the Wildhack-Smith paper compare the normalized amplitude response ratios for the linear and rotational systems:

$$R_{rot} = [(1-2\varepsilon^2)^2 + 4P^2\varepsilon^2]^{-\frac{1}{2}}$$

$$R_{lin} = [(1-\varepsilon^2)^2 + 4P^2\varepsilon^2]^{-\frac{1}{2}}$$

where R = response ratio, the ratio of the dynamic response to the static response,

ε = frequency ratio, the ratio of the test frequency to the natural frequency of the accelerometer, and

P = damping ratio, ratio of the actual damping to critical damping.

These equations show that in the rotational case resonance occurs at a lower frequency and with greater amplitudes than in the case of excitation by linear vibration. In the linear case the maximum response ratio generated is unity for any damping ratio greater than 0.707; in the rotational case it is unity for any damping ratio greater than 1.0. An instrument with damping in the 0.707 to 1.0 range will be easier to analyze graphically in the rotational case since the frequency corresponding to the maximum response ratio can be readily identified.

3. Description of the Calibrator

Based on the theoretical considerations discussed, Smith and Wildhack built a prototype calibrator using a surplus steel shaft and shaft support assembly with ball bearings and a small flywheel. A dc shunt motor was rigidly connected to this shaft; brass slip rings and carbon brushes provided electrical connections to the accelerometer. The device was used to demonstrate the dynamic calibration concept but was not designed for practical calibration service. The drive was not capable of the desired constant speed operation, bearings and slip rings were noisy, it was difficult to balance the system dynamically and the shaft was not rigid enough.

To overcome these shortcomings, the new earth's field dynamic calibrator that is the subject of this report was designed, built and tested. In the new calibrator a dc multiple-pole motor was coupled to the shaft magnetically and this shaft was supported by air bearings. The position of the accelerometer could be adjusted by means of a lead screw and balancing was achieved by means of an adjustable counterweight. The calibrator covers a frequency range of 1/2 to 45 rps. The first resonance of the system occurs at about 22 rps causing an apparent shift in the axis of rotation of the test table; this and other resonances, while creating a slight dc shift, do not materially change the dynamic response of the accelerometer provided the test table does not become appreciably unbalanced. The following paragraphs will describe the new calibrator in detail.

The major components of the earth's field dynamic calibrator are as follows:

(1) "v" block

(2) two air bearings

(3) shaft

(4) test table

(5) driven magnet assembly

(6) slip ring assembly

(7) accelerometer mounting block

(8) counterweight block

(9) drive magnet assembly

(10) motor

Design sketches of the components are shown in the Appendix.

The "v" block supports and aligns the two air bearings which in turn support the shaft in a horizontal position (see Figure 1). The test table is attached to one end of the shaft and the driven magnet assembly is fastened to the other end; the shaft also holds the slip ring assembly, which is a commercial item. The test table holds the accelerometer mounting block and the counterweight block (see Figure 2). The drive magnet assembly is fastened to the motor shaft. The motor shaft and main shaft are magnetically coupled but mechanically isolated.

The test table is symmetrically shaped to facilitate dynamic balancing. When the accelerometer mounting block and counterweight block are attached to the test table, the center of gravity of both blocks lie in the same plane at right angles to the axis of rotation of the test table and symmetrically disposed about the axis. Each block can be moved independently in this plane toward or away from the test table axis of rotation and, when the desired location is reached, tied down securely with screws. The position of each block with respect to the test table axis of rotation is approximately set by means of a depth micrometer. When both blocks are mounted equidistant from the test table axis of rotation, the test table remains in balance.

The shaft is supported by two air bearings; the air bearings have a low coefficient of friction and serve to attenuate extraneous vibration that would degrade the accelerometer output by avoiding shaft to bearing contact. The bearings, commercially available items, have an ID of 1 1/2 inches and are 3 inches long; they required a filtered (10 micron) air supply of 10 to 50 psi.

The driven magnet assembly is a disc with 12 permanent horse shoe magnets mounted radially every 30° along the perimeter (magnetic poles away from the center of the disc); this assembly is attached to the calibrator shaft. The drive magnet assembly is a shallow cylinder that is also equipped with 12 magnets mounted radially (magnetic poles toward the center of the disc); this assembly is attached to the motor shaft. In use, the driven magnet assembly disc is inserted in the drive magnet assembly cylinder so that the magnetic poles of the two assemblies face each other; the motor is thus coupled magnetically to the rest of the calibrator, reducing the transmission of motor vibration to the shaft. An added advantage of this arrangement is that the alignment of the calibrator shaft and motor shaft is not critical. The motor used is a dc multiple-pole type which is capable of low speed operation; an integral optical tachometer produces 2000 pulses for each rotation of the motor shaft so that its speed can be readily monitored.

Supplementary equipment used with the calibrator is as follows:

(1) A variable dc power supply for the motor.

(2) An electronic counter to monitor the rotational speed of the calibrator.

(3) A voltmeter, recorder or oscilloscope for determining accelerometer output.

(4) A power supply for the test accelerometer.

(5) A piezoelectric accelerometer to monitor extraneous calibrator vibration.

(6) A distortion meter to monitor quality of waveform.

4. Transducers Tested

Five different accelerometers were calibrated on the earth's field dynamic calibrator. Three were servo types, one was a semiconductor strain gage accelerometer and one was an unbonded strain gage device. The acceleration ranges represented by these five instruments varied from $\pm 1g$ to $\pm 10g$ while the natural frequencies ranged from 42 Hz to 810 Hz. Table 1 summarizes the pertinent instrument characteristics.

TABLE 1

Instruments Used

Accelerometer	Nominal Natural Frequency Hz	Full Scale Range g	Nominal Output at $\pm 1g$ Peak to Peak volts	Transduction Element	Weight ounces	Size inches
A	700	±1	10	Servo	3.3	1 OD x 1 3/4
B	810	±1	10	Servo	3.3	1 OD x 1 3/4
C	227	±10	1.5	Servo	4.9	3 x 1.5 x 1.4
D	42	±2	0.1	Semiconductor Strain Gage	1.9	1 x 1.1 x 1.8
E	65	±5	0.016	Unbonded Strain Gage	1.3	2.2 x .5 x .5

5. Accelerometer Mounting and Table Balancing Procedures

The accelerometer is mounted on the test table by means of the accelerometer mounting block so that the axis of rotation of the calibrator passes through the center of gravity of the seismic mass for zero acceleration. If the location of the center of the seismic mass is given by the manufacturer, the accelerometer on its mounting block can be set readily by using a depth micrometer and the built in lead screw. Final adjustment can be made with the aid of an oscilloscope; the sinusoidal output of the accelerometer is observed with a dc coupled oscilloscope and if the dc level of the waveform shifts as the speed of the calibration is increased, the location of the accelerometer must be adjusted. The direction of the shift indicates whether the accelerometer should be moved in or out. Since the dc shift is proportional to the square of the rotational speed, the effect will be more pronounced at the higher speeds. Even if the location of the center of the seismic mass is not given by the manufacturer, it can be determined rather quickly by the technique described above.

Since it is important that the test table be in good dynamic balance, the counterweight block must be adjusted in conjunction with the above tests. If the center of gravity of the instrument and its mass are given by the manufacturer, the position of the counterweight block can be

calculated and set by means of a depth micrometer and the built in lead screw (Figure 2). If this information is not given by the manufacturer, a good first approximation is to set both the accelerometer mounting block and the counterweight block at the same distance from the center of rotation of the calibrator.

Visual inspection of the accelerometer waveform on the scope screen at 25-30 Hz is usually sufficient to permit adjustment of the counterweight to a position where calibration can be successfully carried out to at least 20 Hz (the first calibrator resonance occurred at about 22 Hz). If it is desired to generate data up to the maximum speed capability of 45 Hz, additional balancing is generally required; this is done with the use of various lengths of 3/8-24 screws which act as trimming weights. These trimming weights can be screwed into any of the sixteen radial holes located at 22 1/2° intervals around the periphery of the table. A good way of noting the effect of one of these trimming weights is to monitor the unwanted vibrations with a crystal accelerometer (the front air bearing support is a convenient place to mount such an accelerometer). The at-rest noise level of this accelerometer should be well below 0.01g. In addition, a distortion meter can be used to monitor the quality of the waveform; it should be noted that a distortion whose frequency corresponds to the calibration frequency cannot be detected by a distortion meter no matter what the phase relationship.

The various resonances of the calibrator change its apparent axis of rotation, therefore a balancing adjustment that improves the waveform at one frequency may increase the distortion at another frequency. It should be noted that an accelerometer with a natural frequency of 50 Hz will sense considerably less undesirable vibration than another instrument with a 900-Hz natural frequency.

6. Calibration of Three Servo Accelerometers

After all centering and balancing operations for a given accelerometer had been completed, a static calibration was performed with the instrument in place on the calibrator. This was done by placing a precision level on the accelerometer mounting block and adjusting the table so that the accelerometer sensed exactly +1g and then taking a measurement with a precision potentiometer. The table was then rotated 180° and a -1g measurement made (the accelerometer power supply voltage was also measured at this time).

The earth's field dynamic calibrator was then set into motion with the first calibration point being taken at a frequency of 2 Hz (the low frequency limit was not imposed by the calibrator, which can rotate smoothly down to 1/2 Hz, but by the ac voltmeter available). The accelerometer output was measured with a precision, rms ac differential voltmeter (Figure 3 shows the limit of error of this voltmeter as a function of frequency). The 2000 pulses/revolution signal provided by the

tachometer was used in conjunction with an electronic counter to monitor rotation rate. An adjustable dc power supply was used to set the motor speed. Calibrations were made at frequencies from 2 Hz to 24 Hz.

At the conclusion of the dynamic calibration a second static earth's field calibration was performed. The average of the two static calibration values was taken as the reference value with which to compare all dynamic calibrations. All sinusoidal calibration points were corrected for the loading effect due to the input impedance of the readout equipment. For all three servo instruments the agreement between dynamic and static calibrations was found to be within about ±0.5% from 2 Hz to 8 Hz; all were within the limit of error of the voltmeter. The agreement from 10 Hz to 20 Hz was within ±0.1% and at 22 Hz to 24 Hz within ±0.2% (see Table 2, Limit of Error). Figure 3 shows the frequency response of the three servo accelerometers from 2 Hz to 24 Hz.

In addition to the tests just cited, accelerometer A was calibrated to 40 Hz; increased scatter is evident after the first calibrator resonance which occurs at 22 Hz. The data are shown in Figure 4.

TABLE 2

Estimated Limits of Error as Percentages of Output at 1*g* Peak

Uncertainty in the knowledge of the results of the calibrations, comprising the following error components, (assuming the sources of error to be independent), is determined as follows:

Static Calibration		
Potentiometer (two readings per calibration)	±0.010%	
Standard Cell (used twice with potentiometer)	0.005	
Leveling (accelerometer leveled for +1*g* and -1*g*)	0.008	
Sensitivity Drift (estimated)	0.004	
Root sum square error	±0.014%	
Dynamic Calibration		
RMS Differential Voltmeter	±0.100%	(10-30 Hz)
Calibrator Vibration (estimated)	0.250	
Accelerometer Axis Misalignment (estimated)	0.001	
Effect of Rotational Cooling (estimated)	0.070	
Noise Output Instrument A, 0.10% Instrument B, 0.10% Instrument C, 0.48%	See Left	
Root sum square error (dynamic)	±0.30 % ±0.55 %	Instruments A, B Instrument C

7. Calibration of Two Low Frequency Accelerometers

Two low-frequency accelerometers were calibrated in this series of tests: accelerometer D, a semiconductor strain gage device, and accelerometer E, an unbonded strain gage instrument.

The following tests were carried out on accelerometer D:

(1) The waveform was observed with a direct coupled oscilloscope at the following frequencies: 1, 5, 10, 15, 20, 25, 30, 35, 40, and 45 Hz.

(2) Since in many cases waveform distortion is not apparent to the eye until it exceeds about 5%, distortion was measured with a distortion analyzer. Since 20 Hz was the minimum frequency limit of the distortion analyzer used, these measurements were limited to the range 20-45 Hz. The maximum distortion found was 3.8%; the data are shown in detail in Table 3.

(3) A frequency response bar graph (see Figure 5a) was constructed at the frequencies listed in (1). This technique offers the convenience of viewing all 10 frequencies on the same photograph, but does not permit inspection of the waveform. Since in these tests the oscilloscope was direct coupled, the vertical position of each bar on the photograph indicates the presence of any steady g component that exists as a result of the center of the seismic mass of the accelerometer not coinciding with the axis of the center of rotation of the test table. As previously mentioned the center of rotation of the test table changes as the calibrator goes through resonances at several points; this does not, however, measurably affect the amplitude of the individual bar graphs. After the bar graph was completed, it was scaled and plotted; the results are shown in Figure 8. Footnote 2 describes the oscilloscope procedure for constructing a bar graph.

---

[2]The frequency response bar graph was constructed by setting the oscilloscope horizontal display to "Delaying Sweep", the "Delaying Sweep" to 1 ms/cm, and the main sweep to 40 μs/cm. This allowed the display of a trace 0.4 cm wide out of a total width of 10 cm. While rotating the accelerometer at the desired frequency with its output connected to the oscilloscope, the camera shutter was opened for an exposure time of ten seconds (this allowed a sufficient number of scope sweeps to fill in the entire bar or rectangle). The horizontal position of the 0.4 cm trace was then moved 1 cm by means of the "Delay Time Multiplier" and the process repeated for the next frequency.

(4) A continuous calibration from 45 Hz to dc was obtained by rotating the balanced test table holding the accelerometer at 45 Hz and shutting off the power to the electrical motor driving the test table. In this test the accelerometer output was photographed on a direct coupled oscilloscope set to a sweep rate slow enough to record the run down from 45 Hz to dc (see Figure 5b). In this technique it is not possible to identify frequencies precisely on the photograph; they can, however, be identified approximately by noting the test table frequency on a counter as a function of the sweep speed of the oscilloscope. This test allows a complete, continuous calibration from 45 Hz to dc on a single photograph.

Low frequency accelerometer E was subject only to test 3 and 4; the data obtained are shown in Figure 5c, 5d, and 9.

Since low frequency accelerometers D and E both attenuated the higher frequencies, servo accelerometer A was also subjected to tests 1-4 because its higher natural frequency provided a better measure of the quality of the waveform produced by the earth's field dynamic calibrator. Figures 6 and 7 show the waveform of accelerometer A from 1 Hz to 45 Hz, Table 3 shows the distortion and Figure 7 shows the bar graph and continuous calibration data.

TABLE 3

Distortion

Frequency Hz	Accelerometer A Distortion %	Accelerometer D Distortion %
20	0.8	3.8
25	0.4	3.6
30	0.7	3.0
35	1.7	2.0
40	2.8	1.2
45	3.8	1.8

8. Natural Frequency and Damping as Determined by Rotational and Linear Calibration

The natural frequencies of all three servo accelerometers tested (accelerometers A, B and C) were well above the maximum capability of the earth's field dynamic calibrator; the two strain gage accelerometers (accelerometers D and E) were selected, however, so that amplitude frequency response curves could be constructed. The values of natural frequency and damping as determined with the earth's field dynamic calibrator for the two strain gage accelerometers (D and E) did not agree with the values determined on the electromagnetic shaker. Figures 8 and 9 show the differences.

Part of the discrepancy is explained as follows: it was previously shown that the accelerometer's seismic mass could be centered to coincide with the test table axis of rotation by observing the accelerometer's output on a direct coupled oscilloscope. This centers the seismic mass along the sensitive axis only. If, as is often the case, the location of the center of the seismic mass is not given by the manufacturer, there is no ready way of knowing the location of the seismic mass along the transverse axis. Consider for example accelerometer D which has a cylindrical seismic mass that is supported by a cantilever spring as is shown in sketch (a) below. If the instrument is re-mounted as in sketch (b) below, the "spring constant" of the spring mass system is increased and the natural frequency of the instrument increased by the effect of the centrifugal field of the calibrator test table; in sketch (c) the "spring constant" of the system is decreased and the natural frequency of the instrument lowered by the effect of the centrifugal field of the calibrator test table. Obviously it is not desirable to get a different answer for every position of the accelerometer (seismic mass) on the calibrator test table. Figure 10 shows how the apparent natural frequency was altered by the transducer's position on the calibrator test table. In this particular case the effect can be reduced or eliminated by rotating the accelerometer (seismic mass) 90° and remounting; the seismic mass could then have positions such as in sketches (d), (e) or (f). Figure 10 also shows how the data for positions (a), (d) and (e) yields the same value of natural frequency and damping; the instrument was not tested in position (f).

The results obtained with the transducers in positions (a), (d) and (e) were consistent, but still did not agree with the values of natural frequency and damping determined on the electromagnetic shaker. The reasons for the remaining discrepancies are not known at this time.

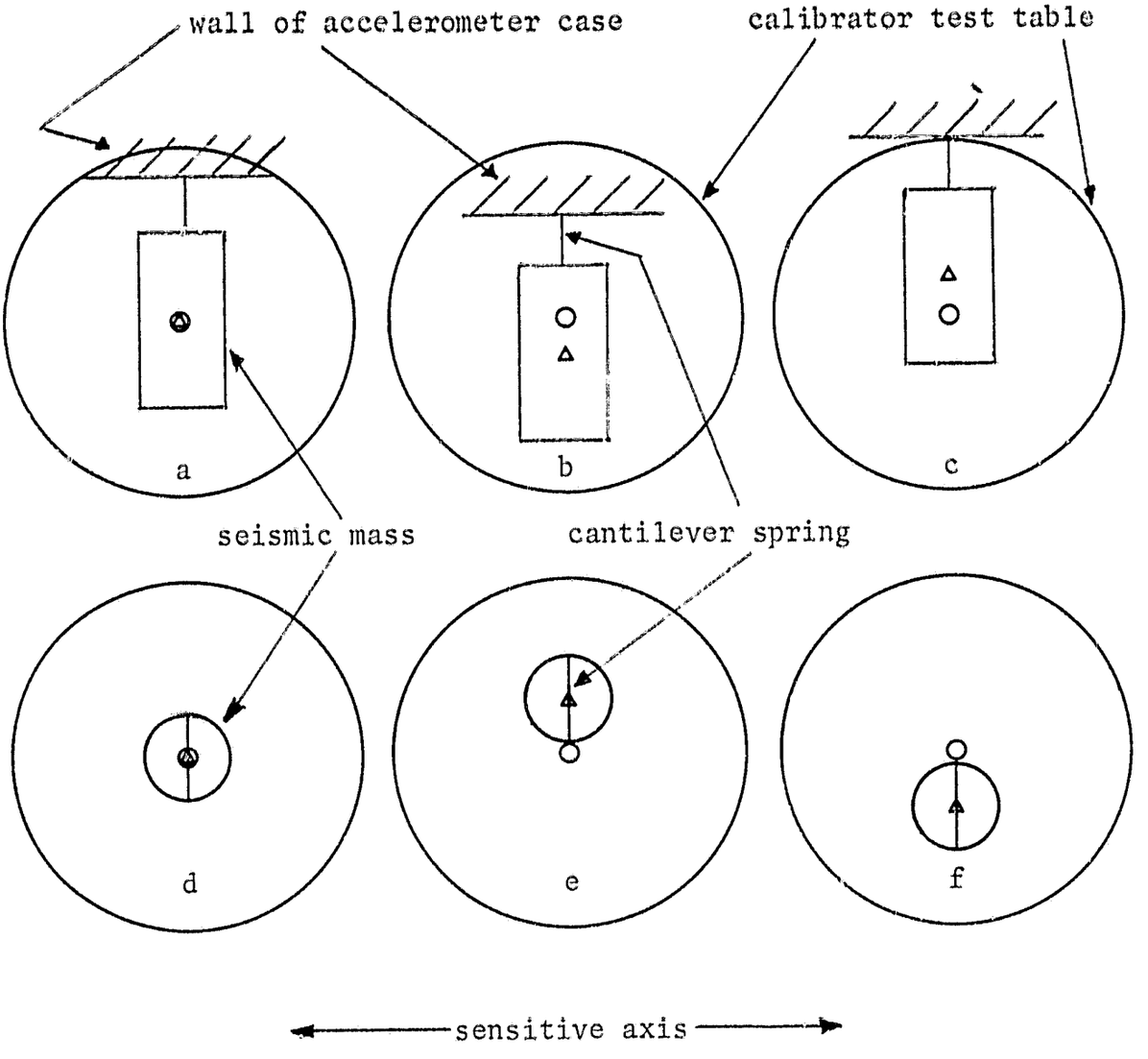

○ center of rotation of calibrator test table
△ center of gravity of seismic mass

9. Summary

An Earth's Field Dynamic Calibrator was built and evaluated. The calibrator rotates an accelerometer (sensitive axis in a vertical plane) about a horizontal axis in the earth's gravitational field at steady speeds ranging from 1/2 to 45 revolutions per second, thus generating a $\pm 1g$ (9.80665 m/s^2) peak sinusoidal acceleration. The calibrator features air bearings and a magnetic drive.

Three high-natural-frequency servo accelerometers have been calibrated from 2 Hz to 24 Hz. The agreement between the sinusoidal excitation responses and the static response was within ±0.1% from 10 Hz to 20 Hz, ±0.2% from 22 Hz to 24 Hz and ±0.5% from 2 Hz to 8 Hz (the deviations from perfect agreement are attributed largely to accuracy limitations of the voltmeter used).

Two low frequency strain gage accelerometers have been calibrated from 1 Hz to 45 Hz. It was demonstrated that the apparent natural frequency and damping of an accelerometer depend on the location of the center of gravity of the seismic mass with respect to the axis of rotation of the calibrator. This suggests that in practical use such an accelerometer used to make a measurement in a rotating situation may give erroneous information.

10. Conclusions

The earth's field dynamic calibrator has been found to be superior to the electromagnetic shaker for the dynamic calibration of precision high frequency accelerometers, such as servo-types. This calibrator offers improvement in the present state of the art of dynamic calibration of accelerometers; static and dynamic calibrations of several accelerometers were found to agree within ±0.1% at frequencies between 10 and 20 Hz.

The carefully confirmed discrepancies between experimentally determined values of natural frequencies and damping ratios for linear and rotational dynamic calibrations of low-natural-frequency accelerometers indicate that the rotational technique should be avoided or used only with great caution for accelerometers of that type.

The author gratefully acknowledges the technical assistance of Paul S. Lederer, Leon Horn, Dr. Daniel Johnson, Randolph Williams and Kurt Muhlberg in the design, construction and evaluation of the earth's field dynamic calibrator.

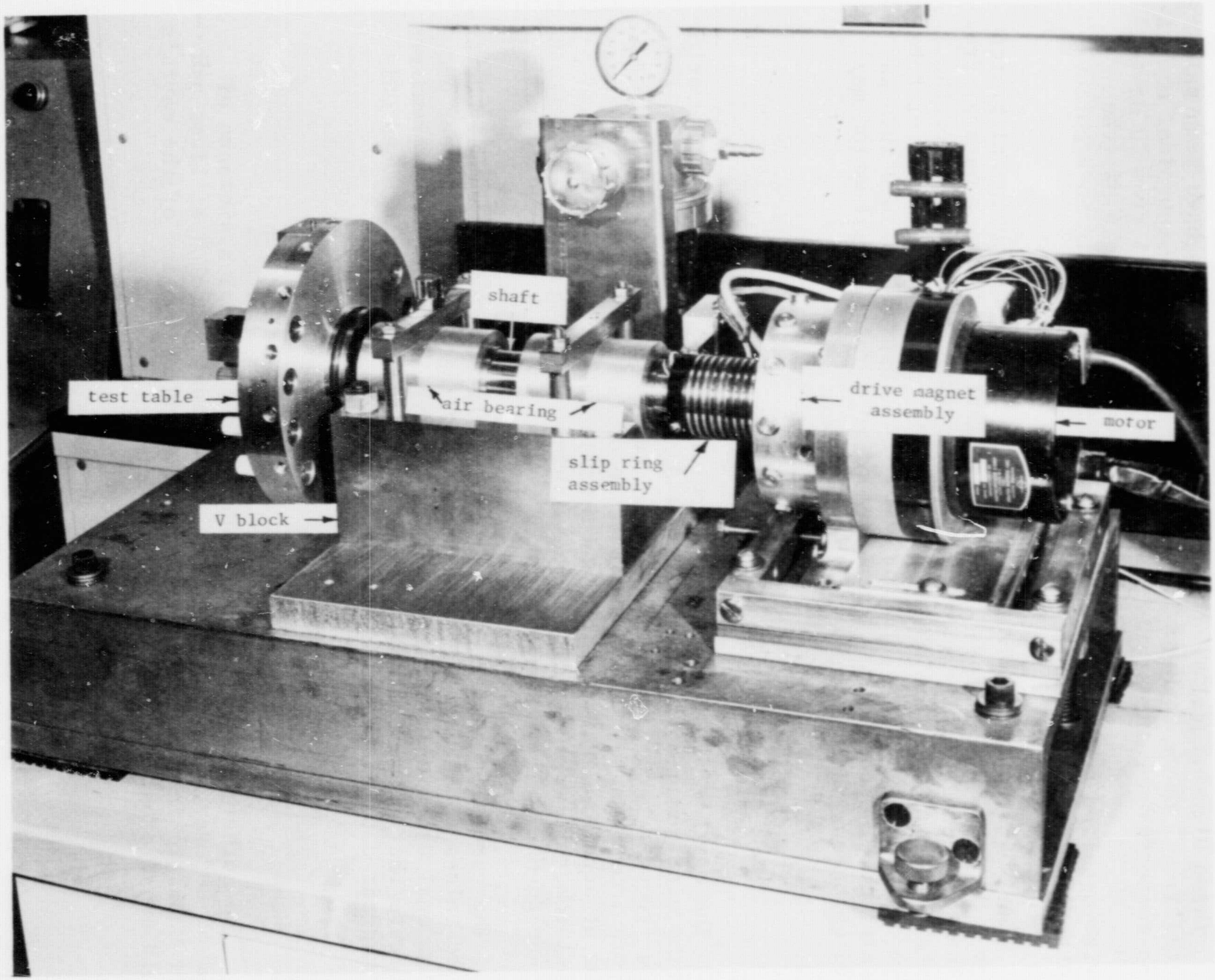

FIGURE 1: EARTH'S FIELD DYNAMIC CALIBRATOR

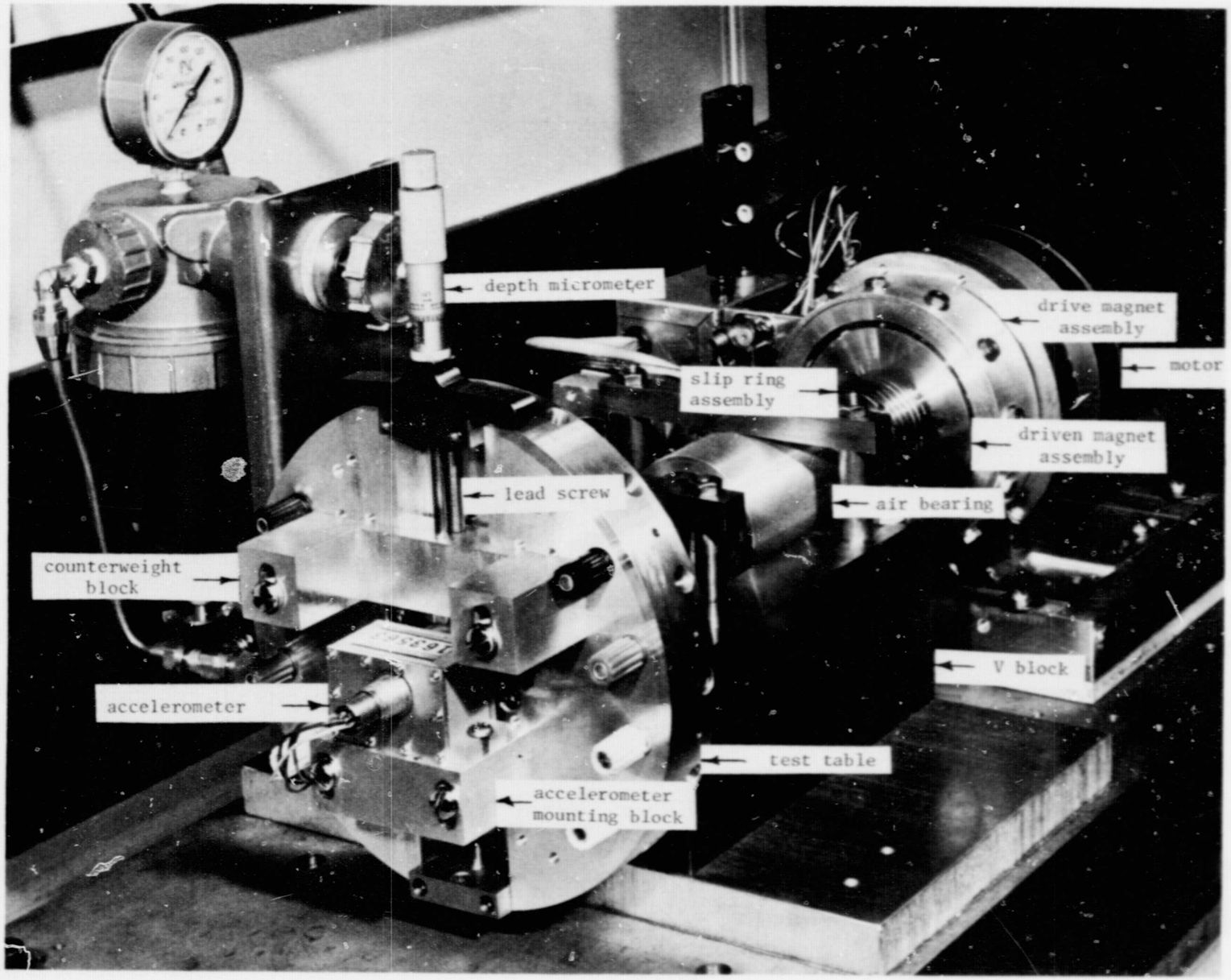

FIGURE 2: EARTH'S FIELD DYNAMIC CALIBRATOR

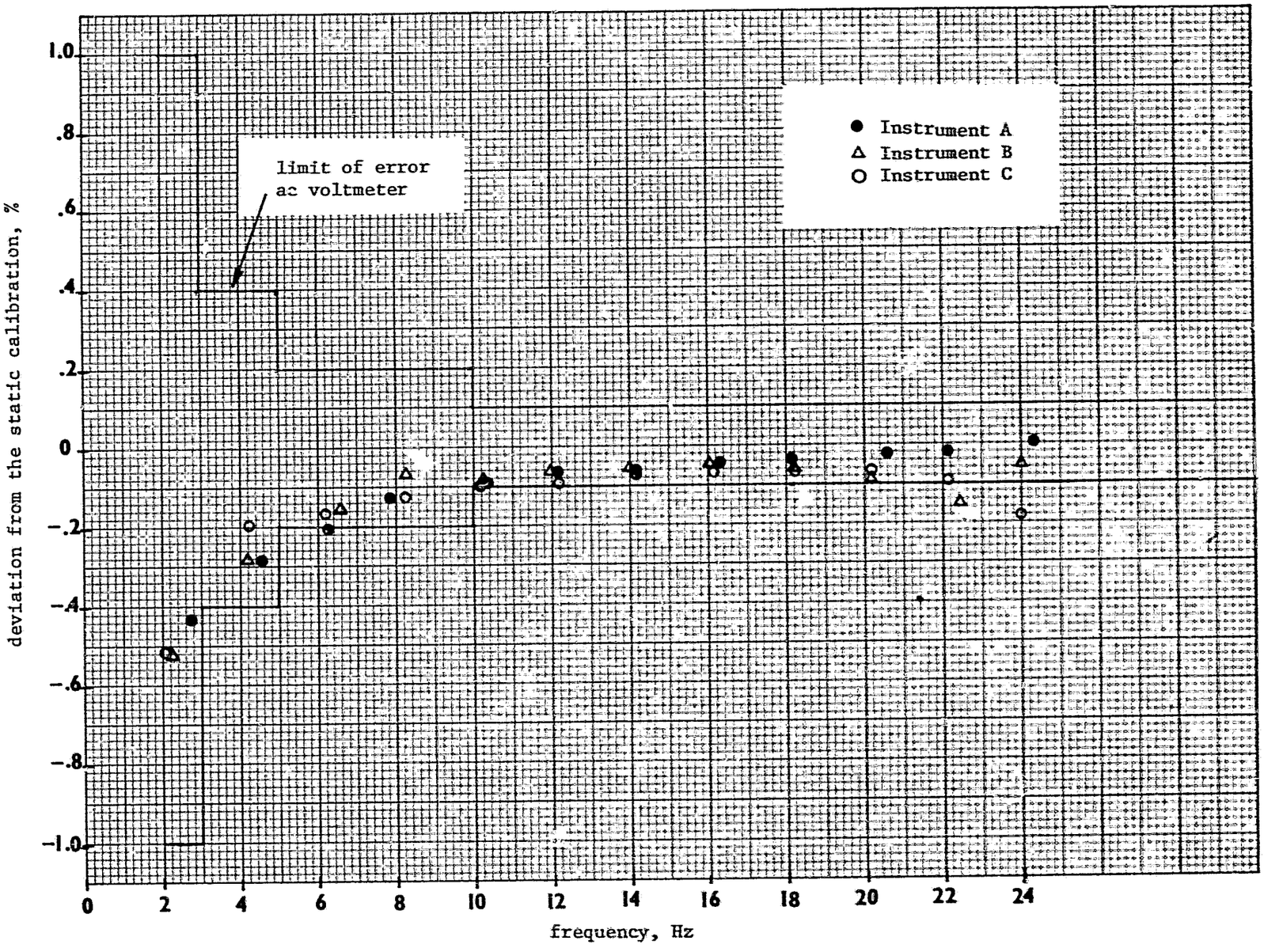

FIGURE 3: CALIBRATION OF THREE SERVO ACCELEROMETERS

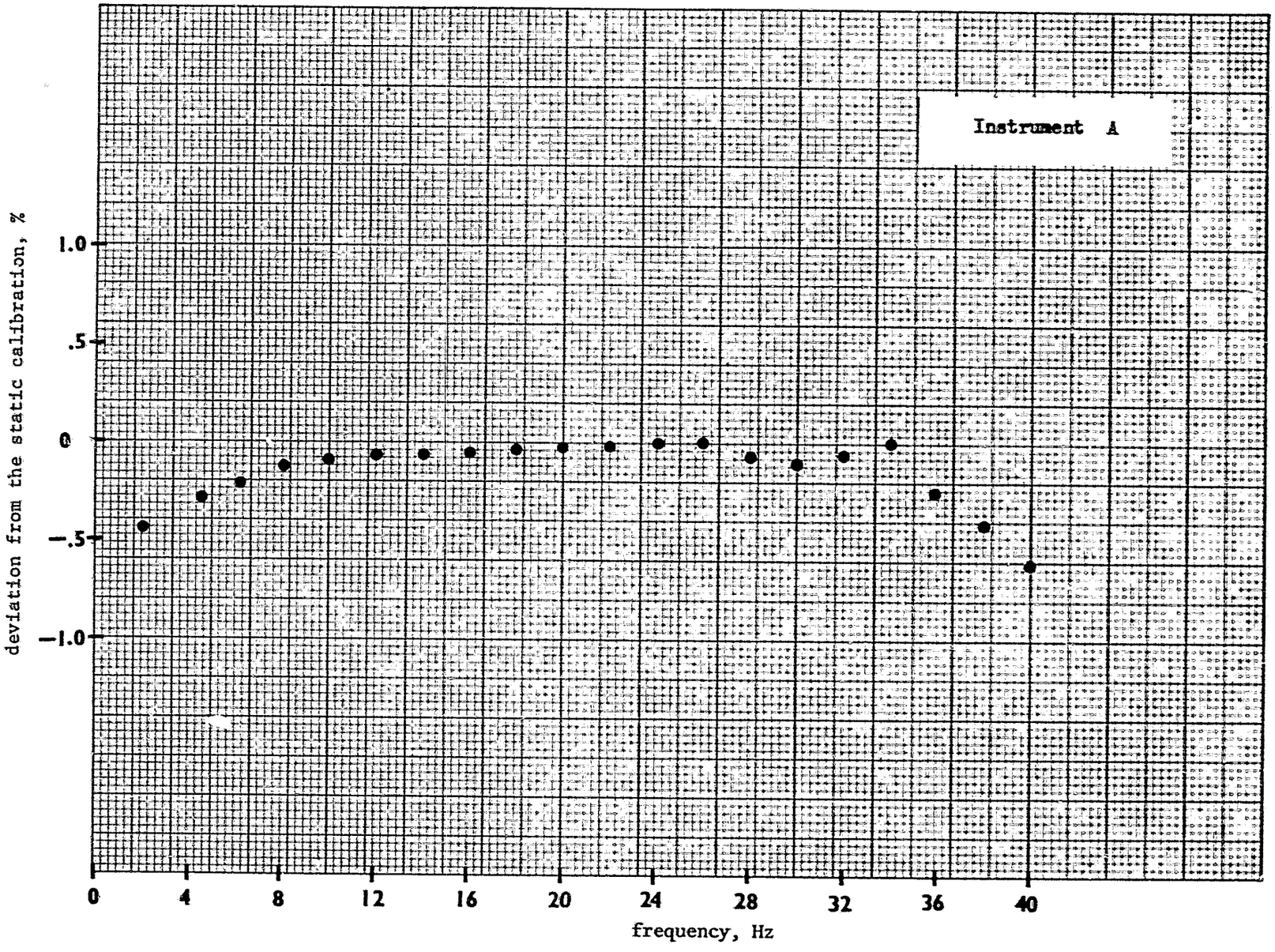

FIGURE 4: HIGH FREQUENCY CALIBRATION OF SERVO ACCELEROMETER A

5 (a)

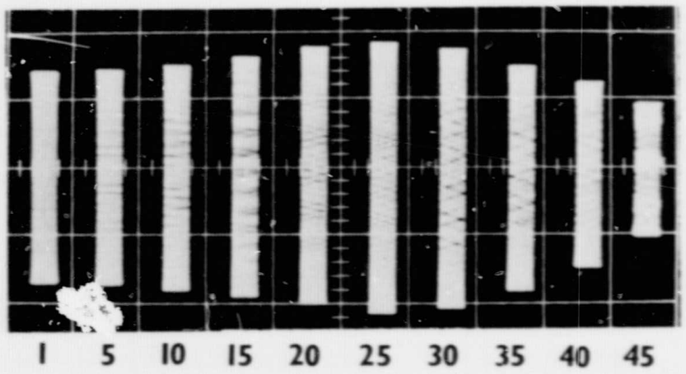

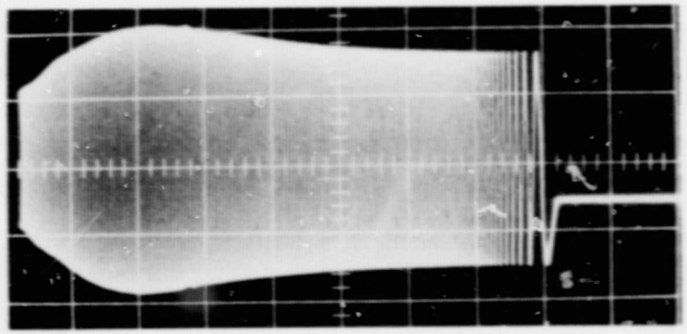

5 (b)

FREQUENCY RESPONSE, ACCELEROMETER D

5 (c)

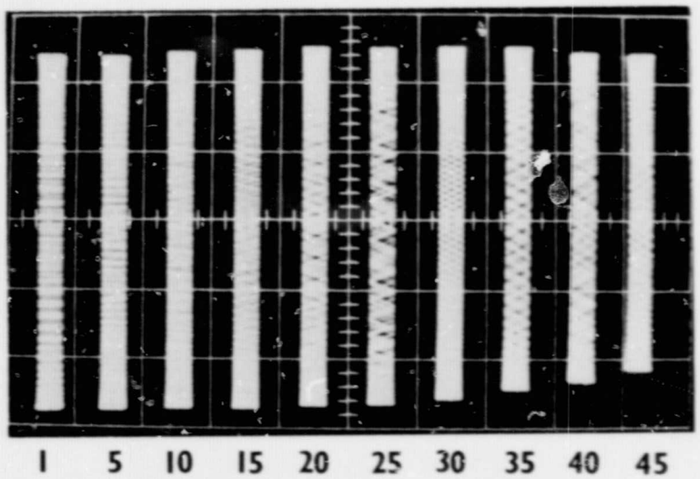

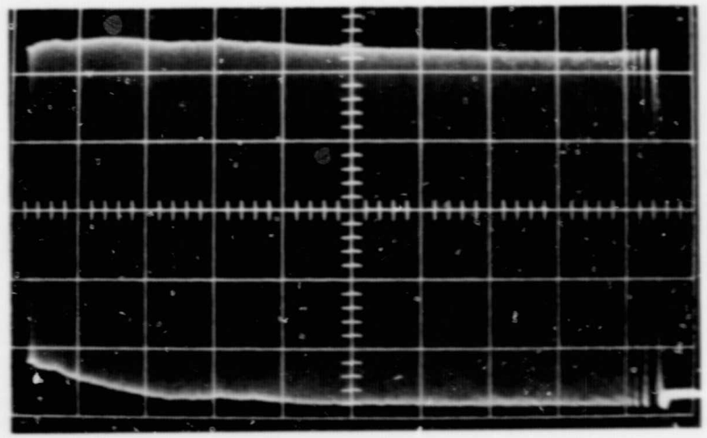

5 (d)

FREQUENCY RESPONSE, ACCELEROMETER E

FIGURE 5: FREQUENCY RESPONSE, ACCELEROMETER D AND ACCELEROMETER E

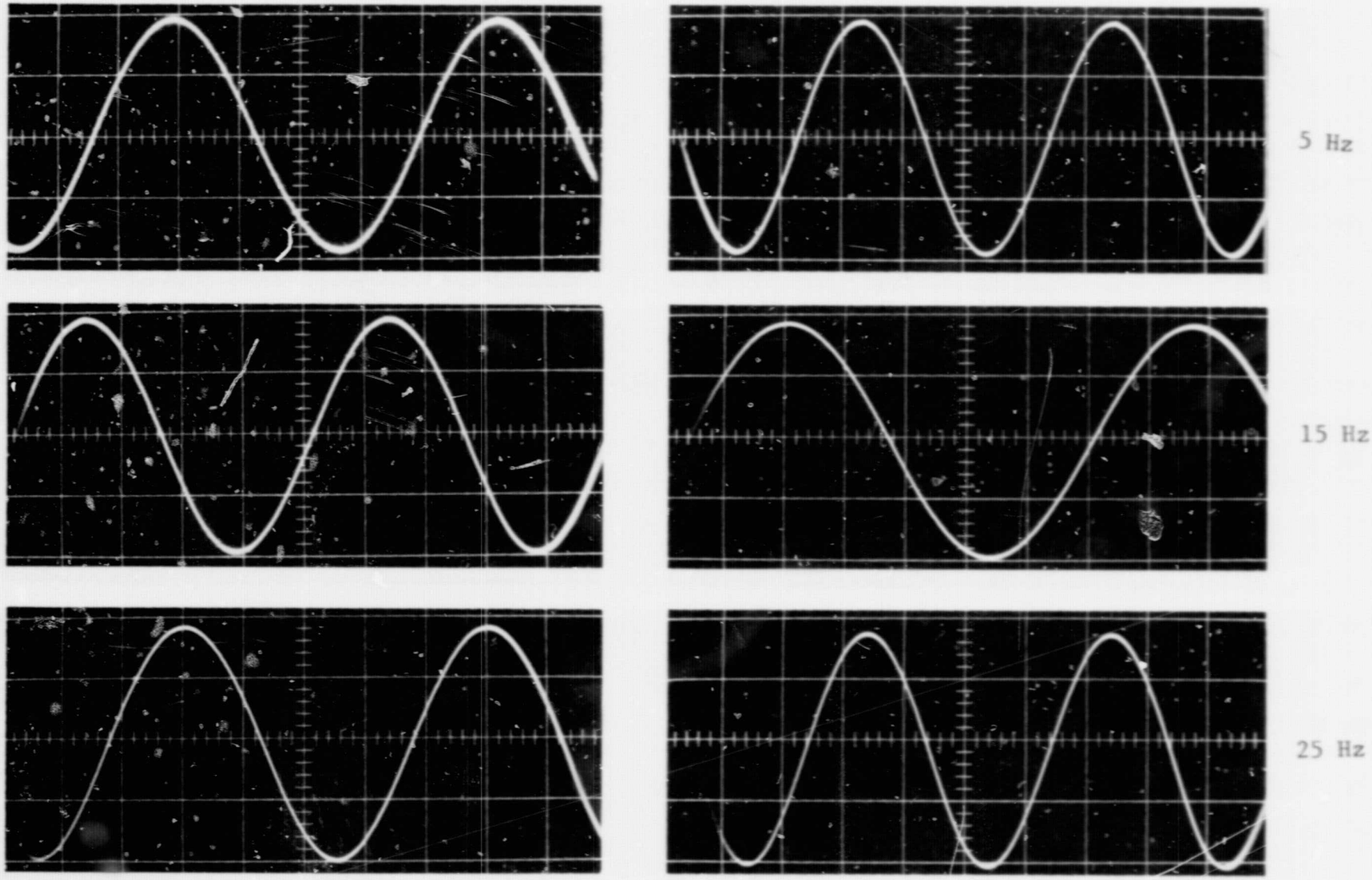

FIGURE 6: SERVO ACCELEROMETER A WAVEFORM

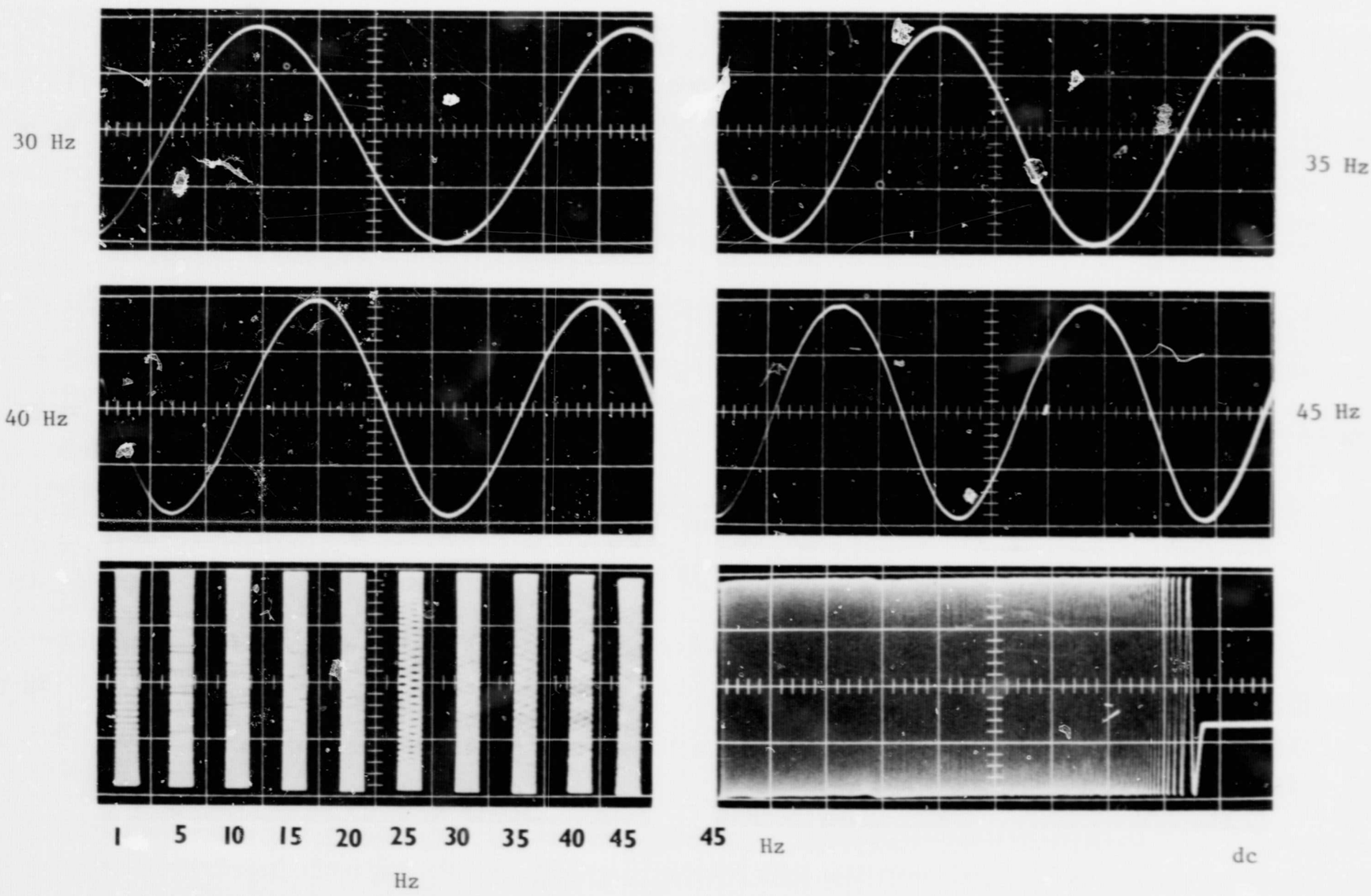

FIGURE 7: FREQUENCY RESPONSE SERVO ACCELEROMETER A

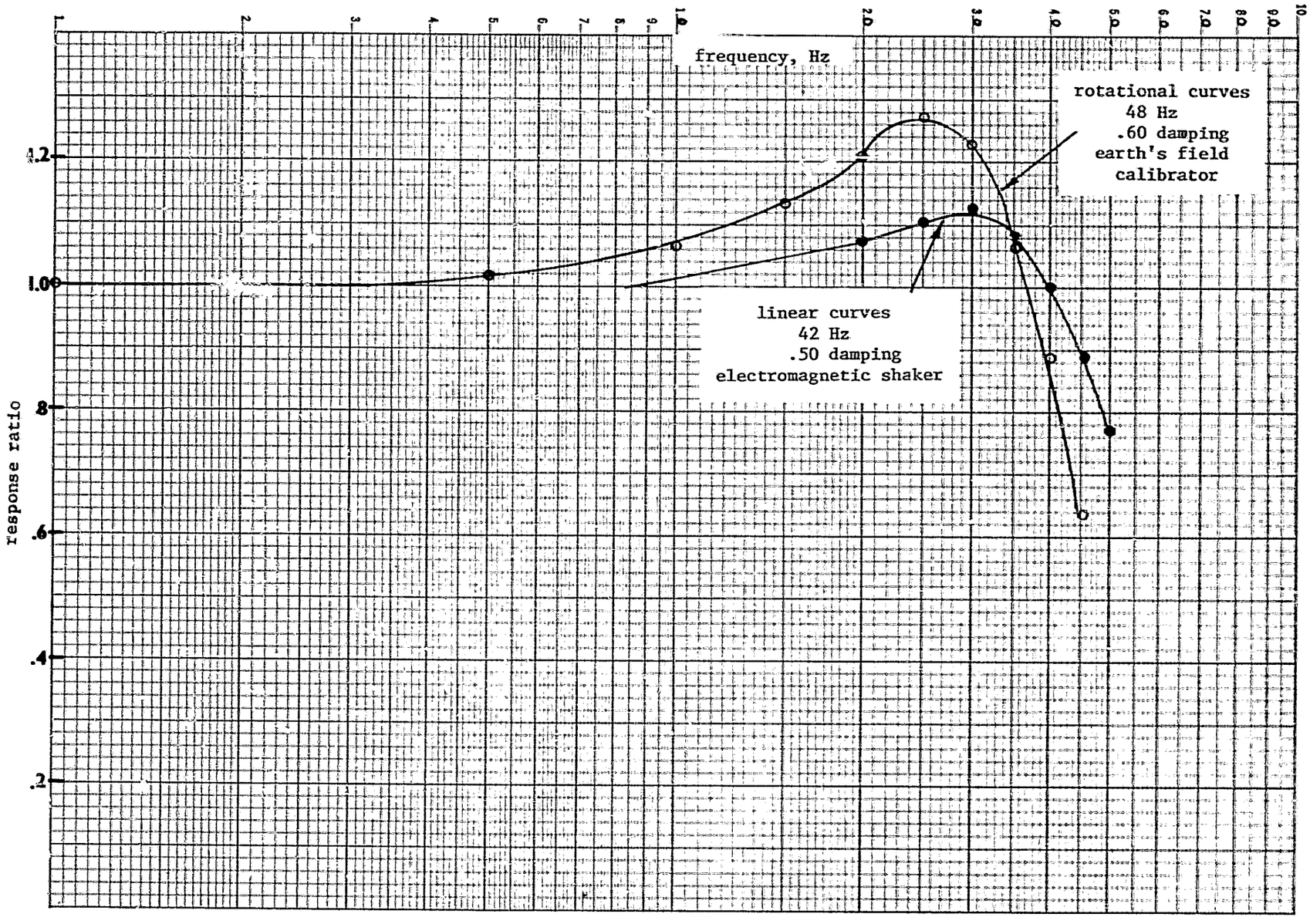

FIGURE 8: LINEAR AND ROTATIONAL FREQUENCY RESPONSE, (ACCELEROMETER D)

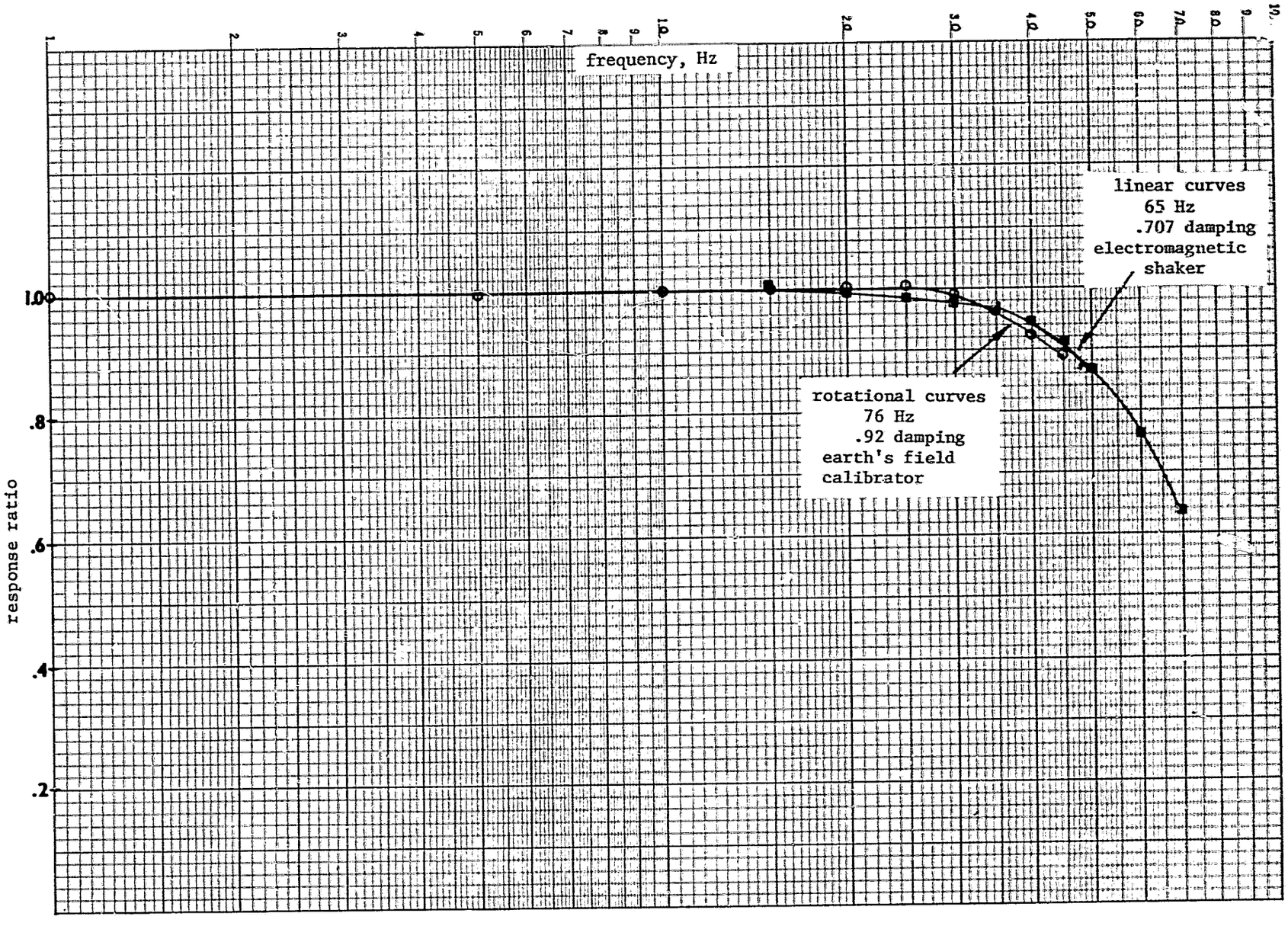

FIGURE 9: LINEAR AND ROTATIONAL FREQUENCY RESPONSE, (ACCELEROMETER E)

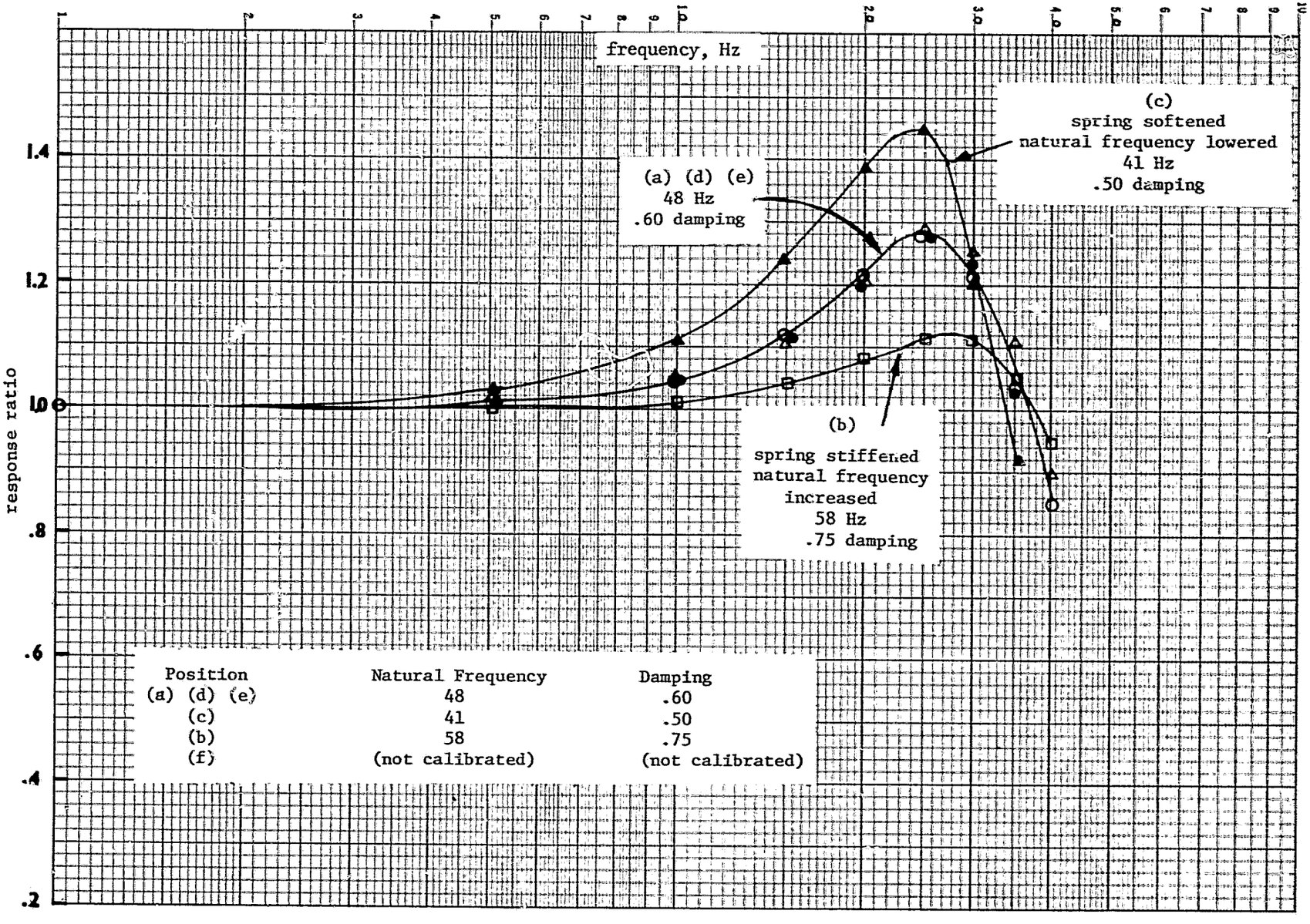

FIGURE 10: FREQUENCY RESPONSE OF ACCELEROMETER D AS A FUNCTION OF PLACEMENT ON CALIBRATOR TEST TABLE

11. Appendix

Figures A1 - A4 show simplified drawings of the major mechanical components that constitute the earth's field dynamic calibrator described in this report. These components are (1) the test table, (2) the shaft, (3) the v-block assembly, and (4) the motor and magnet assemblies.

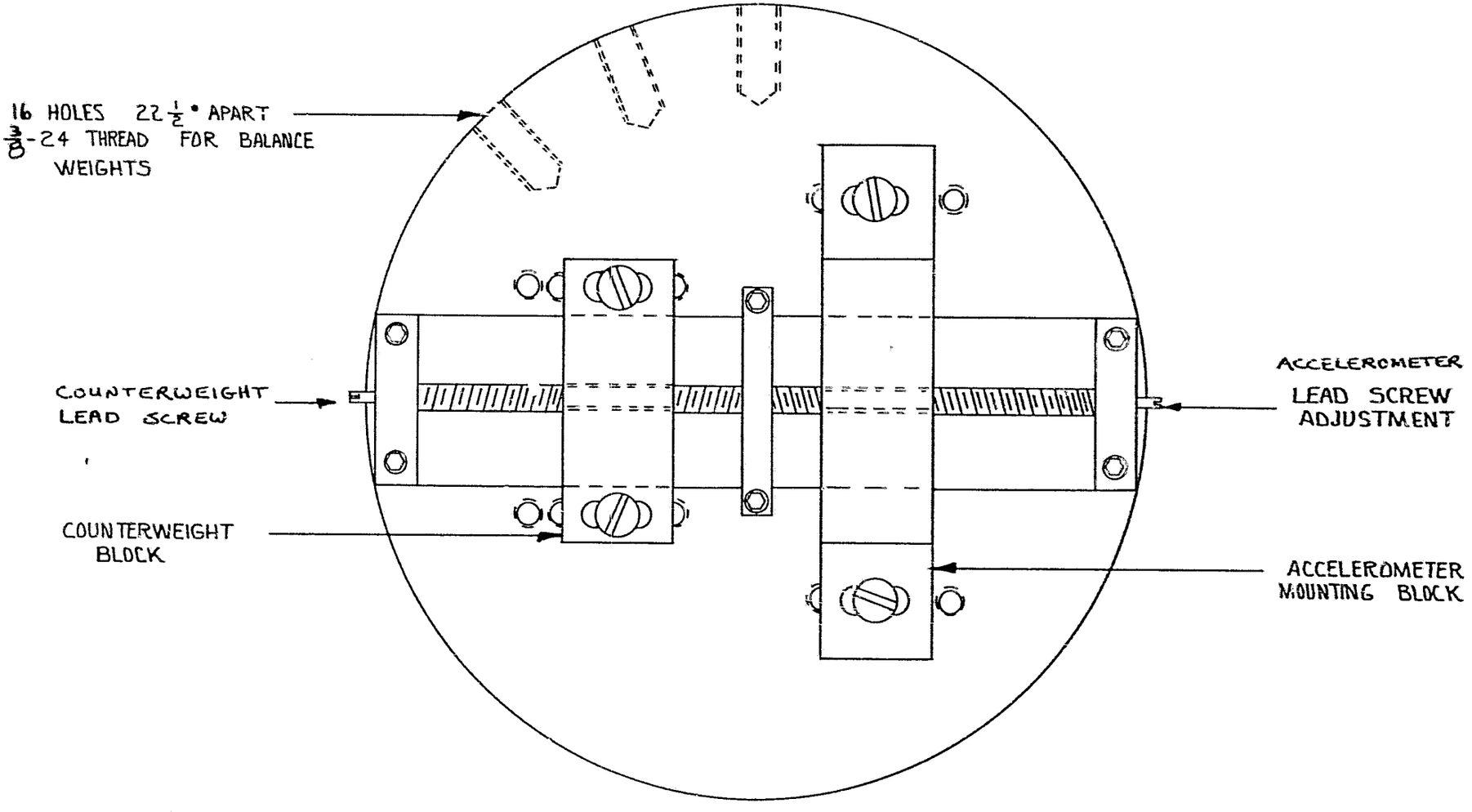

FIGURE A1: TEST TABLE

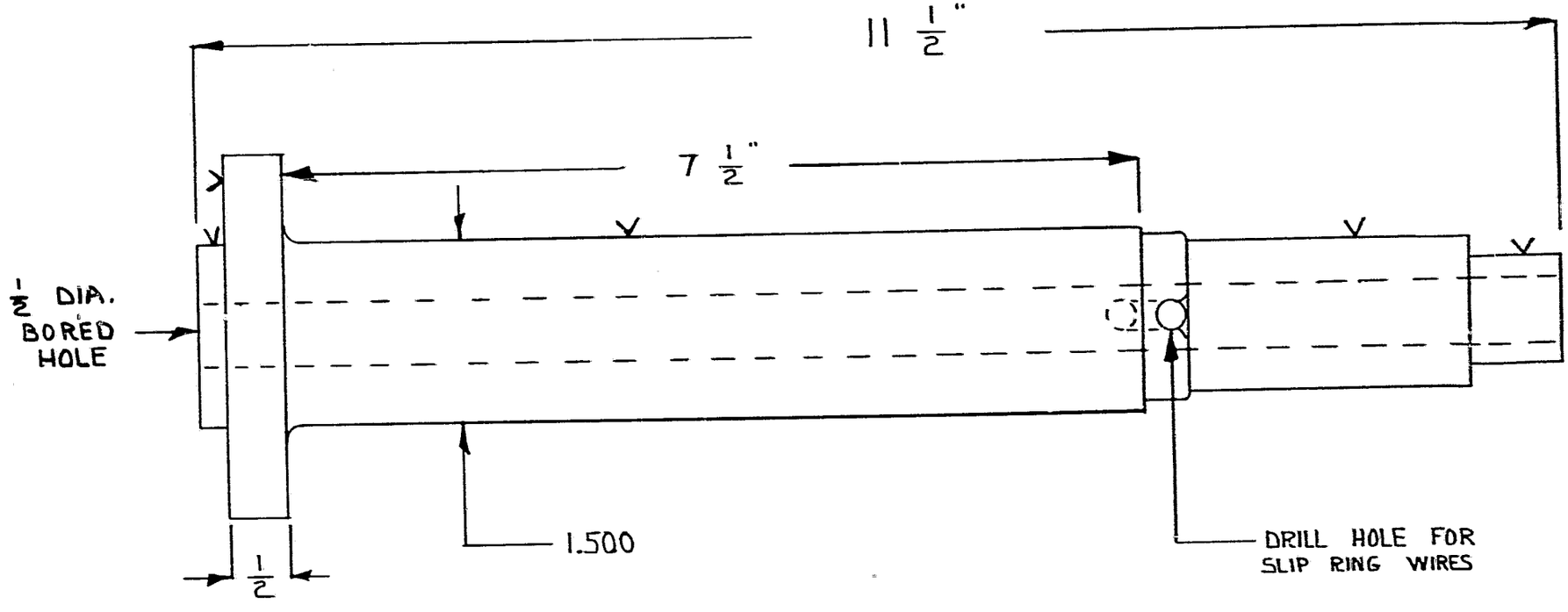

MATERIAL — AISI 02
HEAT TREAT ROCKWELL 61
FINISH (V) 16 MIC. IN.

FIGURE A2: SHAFT

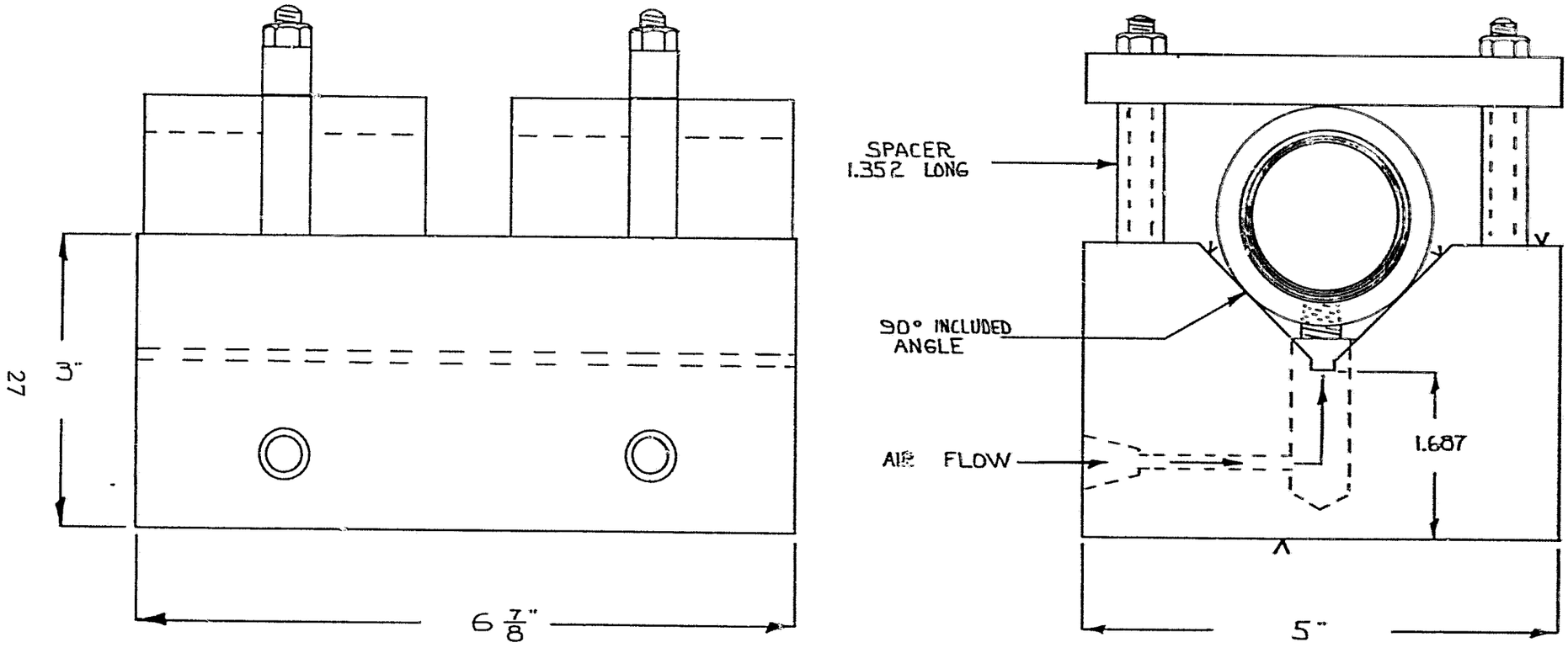

MATERIAL — AISI 02
HEAT TREAT ROCKWELL 61
(v) FINISH 16 MIC. IN.

FIGURE A3: V-BLOCK ASSEMBLY

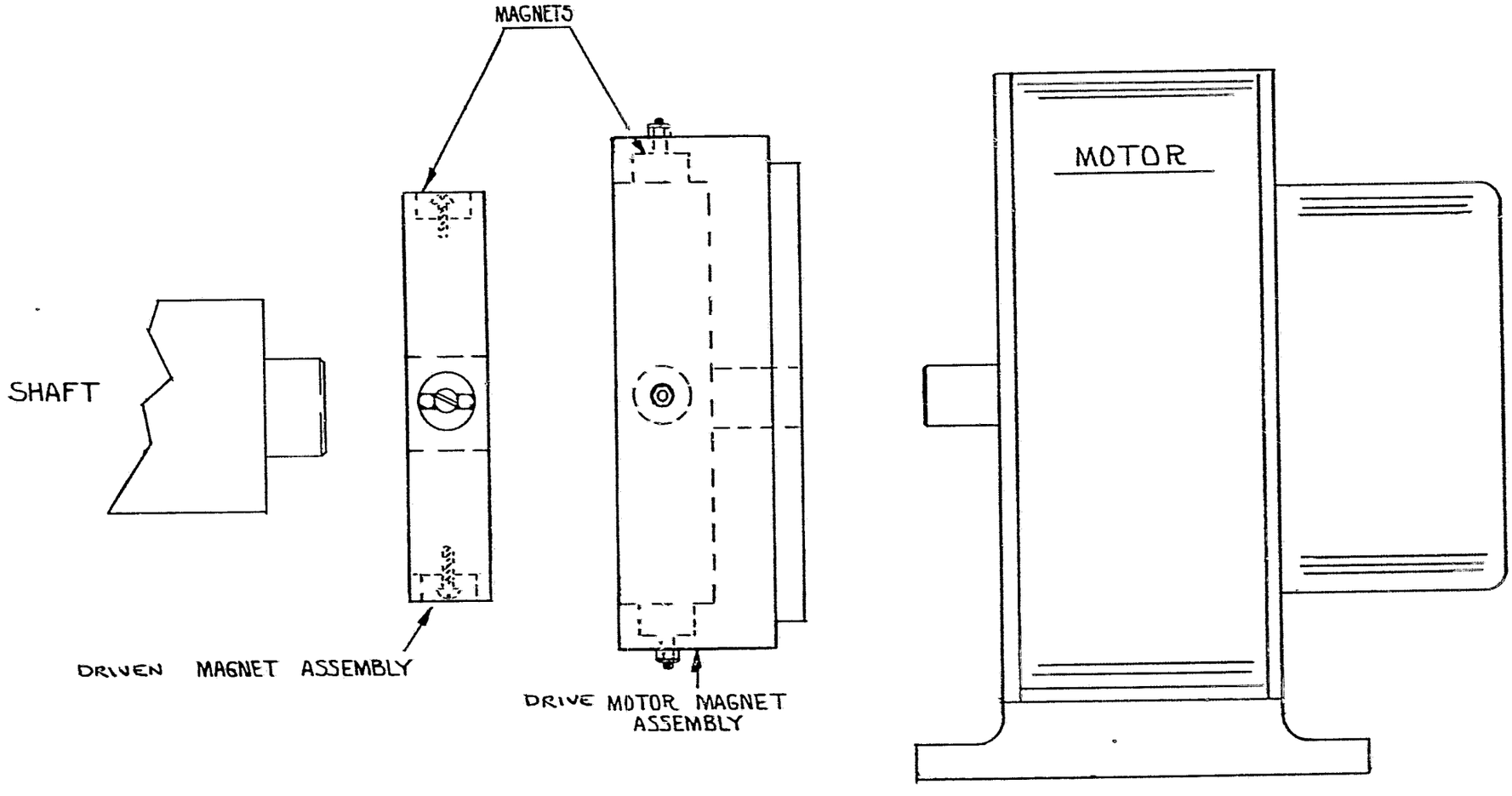

FIGURE A4: MOTOR AND MAGNET ASSEMBLIES